ELSEVIER

Thermochimica Acta 320 (1998) 23–32

thermochimica acta

Soot deep oxidation catalyzed by molybdena and molybdates: a thermogravimetric investigation

M.A. Hasan, M.I. Zaki*, K. Kumari, L. Pasupulety

Chemistry Department, Faculty of Science, Kuwait University, P.O Box 5969, Safat, 13060, Kuwait

Received 25 March 1998; received in revised form 8 June 1998; accepted 16 June 1998

Abstract

Molybdena (MoO_3) and molybdates of bismuth ($Bi_2Mo_3O_{12}$), chromium ($Cr_2Mo_3O_{12}$), barium ($BaMoO_4$), manganese ($MnMoO_4$) and copper ($Cu_3Mo_2O_9$) were synthesized and characterized by X-ray powder diffractometry and infrared spectroscopy. They were then assessed as 'loose contact' catalysts for soot deep oxidation (combustion) in air by thermogravimetry. A similar assessment was carried out on commercial chromia (Cr_2O_3) and tungsta (WO_3). Observed high oxidation activity of MoO_3, as compared to both Cr_2O_3 and WO_3, is attributed to the higher volatility (mobility) of MoO_x species. On similar grounds, observed high activity of MoO_3 and $Cu_3Mo_2O_9$, as compared to the other test molybdates, is explained. Relatively speaking, however, a higher activity was observed for $Cu_3Mo_2O_9$ than MoO_3, whereby soot ignition temperature decreased from 571°C (uncatalyzed oxidation) to 430°C, to occur within the temperature range of diesel exhaust (200–450°C). This observation is ascribed to copper-promoted redox conduct of Mo(VI) in the oxidation reaction of soot. Kinetics of the reaction was studied non-isothermally, and the kinetic parameters (A, k, ΔE and the reaction order) were calculated. © 1998 Elsevier Science B.V.

Keywords: Molybdena; Molybdates; Soot; Soot oxidation; Soot oxidation catalysts; Thermogravimetry

1. Introduction

The awareness of the detrimental effects of automotive exhaust emissions to the environment has turned a great deal of research work to the area of catalytic deep oxidation (combustion) of the emitted harmful gases (e.g., CO, NO and hydrocarbons) [1–3] and soot particulates [4–7]. The invention and application of the so-called three-way catalyst [1,3], which is composed essentially of Pt and Rh metal particles dispersed on Al_2O_3 surfaces, has lowered the harmful gas emissions of gasoline-powered engines to acceptable levels. Intensive research endeavours have successfully tackled application problems of the catalyst, such as the Rh particle oxidative degradation [8,9], thus improving the catalyst durability. However, this catalyst does not suit emissions of diesel-powered engines, for it functions at higher temperatures ($\geq$650°C) than the temperature range of the diesel exhaust (typically 200–450°C [7]). Consequently, the search was oriented to oxidic materials those are capable of tackling diesel emissions (much richer than the gasoline emissions is soot particulates and unburned large aromatics) [2,3] at low temperature regimes.

The uncatalyzed combustion of soot occurs at higher temperatures (550–650°C) than the diesel

*Corresponding author. Tel.: +965-481-1188/5606; fax: +965-481-6482; e-mail: zaki@kuc01.kuniv.edu.kw

PII S0040-6031(98)00425-0

exhaust temperature [7]. Reportedly, PbO, Co_3O_4, V_2O_5, MoO_3 and CuO [10], copper vanadate [11], and perovskite type oxides [5], are active soot oxidation catalysts. However, VO_x/Al_2O_3 [12] and MoO_x/TiO_2 [13] promoted with KCl and $CuCl_2$ have been found to be more capable of bringing the ignition temperature of soot down to the range of interest (near 400°C). The salt additives have been considered [7] to improve the catalyst volatility (mobility), by leading to the formation of Cu_2OCl_2 and CuCl species. This has been claimed [7] to facilitate a closer contact between the catalytic species and soot particulates. However, there are two important application problems of catalysts based on Copper (oxy) chloride: (i) deactivation by evaporation and/or decomposition of the active compound [7,12,13], and (ii) the possibility that carbon–chlorine bonds are formed (as in the oxychlorination reaction) which by further reaction with oxygen result in formation of very toxic compounds such as chlorobenzenes and chlorophenols [7]. Consequently, Mul et al. have advised the search for other possibilities to eliminate the contamination of the environment by diesel soot particulates, like oxidic catalysts with 'loose contact' activity, fuel additives, or technical developments.

The present thermogravimetric investigation explores the conduct of unsupported molybdena and molybdates of barium, copper, manganese, bismuth and chromium, as soot oxidation catalysts. The exclusion of preparations in the supported form was to avoid reducing the thermal conduction of the catalyst material. On the other hand, the exclusion of using halide compounds of the counter ions was to avoid increasing the catalyst volatility (i.e. avoid deactivation) and detrimental impacts on the environment. MoO_x species enjoy reasonably high volatility (mobility) at the temperature range of interest [14] which can warrant sufficiently close soot/catalyst contact without halide additives. In a series of recent studies [15,16] molybdena structures have been found highly susceptible to mechanical activation (by grinding or milling) which leads to an increased internal energy caused by the generation of coordinatively unsaturated Mo(V). Exposure of such sites at surfaces of molybdena should improve its oxygen chemisorption [16], as well as the mobility and oxidation activity of the resulting surface species [17]. Broadly speaking, chemisorbed oxygen species are capable of deep oxidation, whereas lattice oxide sites can only catalyze selective oxidation [18].

For comparison purposes, the investigation was extended to include oxides of chromium and tungsten. These oxides are also of Group(VI) metals, and their metal atoms also may acquire variable oxidation states in the range (II–VI).

2. Experimental

2.1. Catalysts

Molybdena (MoO_3) was obtained, according to Ismail et al. [19], by calcination (heating in air) of 99.9% pure FLUKA ammonium paramolybdate ($H_{24}Mo_7N_6O_{24}\cdot 4H_2O$) at 450°C for 3 h. Molybdates of copper, barium, manganese, bismuth and chromium were prepared by a similar calcination (450°C, 3 h) of the residues of drying at 100°C (for 48 h) of mixed aqueous solutions of the nitrate compound of the counter cation (AR-grade, MERCK products) and the paramolybdate. The solutions were equimolar and of equal volumes (20 ml), and were maintained with continuous stirring for 1 h at room temperature, prior to drying. The resulting molybdates are indicated below by the chemical symbol of the counter ion. Thus, for instance, $CuMoO_x$ denotes the copper molybdate, and $BiMoO_x$ the bismuth molybdate. The catalysts, ground to particle sizes $\leq$44 μm, were kept dry over silica gel until further use.

Chromia (α-Cr_2O_3) and tungsta (WO_3) were 99% pure products of BDH. Prior to application, these oxides were also ground to particle sizes $\leq$44 μm and kept dry over silica gel.

2.2. Catalyst characterization

Following preparation, the catalysts were characterized by means of X-ray powder diffractometry (XRD) and infrared spectroscopy (IR). XRD was carried out at room temperature, using a Siemens D5000 diffractometer (Germany) equipped with Ni-filtered Cu K_α radiation (λ=0.15418 nm, 40 kV, 30 mA), in the 2θ range between 10° and 80°, with a divergence slit of 1°. The diffractograms, recorded stepwise (step size=0.02°, step time=15 s), were acquired and handled with an on-line microcomputer.

For phase identification purposes, automatic JCPDS library search (standard SEARCH software) and match (standard DIFFRAC AT software) were employed.

IR absorption spectra were taken from KBr-supported test samples (<1 wt.%), over the frequency range 4000–400 cm^{-1}, using a model 2000 Perkin–Elmer FT spectrophotometer (UK). An on-line data station facilitated spectra acquisition and handling.

2.3. Thermogravimetry of soot oxidation

Uncatalyzed and catalyzed soot oxidation in a dynamic gas atmosphere (50 cm^3/min) of air (dry and wet) was followed thermogravimetrically, using automatic TGA-50 Shimadzu analyzer (Japan) equipped with on-line TA-50WS work station for data acquisition and handling. TG (and DTG) curves were recorded while heating the reaction powder mixture up to 700°C at variable heating rate (ϕ=10–50°C/min). The fact that the chosen heating rates are rather high is to accomplish conditions relevant to combustion.

The reaction mixture was prepared by first tumbling and, then, grinding in an agate mortar for 30 min a mixture (at 2:1 weight ratio) of the catalyst and soot (Printex-U, a flame soot obtained from Degussa, Germany) diluted with SiC in order to prevent thermal runaways [7]. The resulting mixtures were examined in the loose powdered form, in order to avoid milling and compaction, and, hence, formation of 'tight contact' catalysts [7]. According to the manufacturer, the soot contains low amounts (total of <5 wt.%) of polyaromatic hydrocarbons, surface oxygen, and nitrogen and sulfur compounds. Typically, about 4±1 mg catalyst, 2±1 mg soot, and 54±1 mg SiC were applied as test sample. Mixture samples containing no catalyst, were composed of 2±1 mg soot and 58±1 mg SiC, in order to maintain the total weight of the mixture constant (60±1 mg). Whether catalyzed or uncatalyzed, the oxidation product of soot was completely volatile and found by means of gas chromatography to be dominated (98%) by CO_2. A similar observation was made by Mul et al. [7].

Non-isothermally measured kinetic parameters, namely, reaction activation energy (ΔE), order (n), frequency factor (A), and rate constant (k), for the weight loss process monitoring the soot deep oxidation ($C_{(s)} \rightarrow CO_{2(g)} \uparrow$), were determined by means of an automatic data treatment in the work station, implementing the mathematical apparatus of Ozawa's method [20]:

$$\log \phi_1 + 0.4567 \frac{\Delta E}{RT_1} = \log \phi_2 + 0.4567 \frac{\Delta E}{RT_2} \tag{1}$$

for determination of ΔE from the slope of $\log \phi$ vs. $1/T$ plots [21]:

$$G(x) \equiv A\theta = \frac{1}{n-1}\left[(1-x)^{1-n} - 1\right], \quad \text{for } n > 1 \tag{2}$$

$$G(x) \equiv A\theta = -\ln(1-x), \quad \text{for } n = 1 \tag{3}$$

where x is the fraction of reaction completed, and θ the reduced time (Ozawa's definition [21]) at x (*for determination of n and A*);

$$t = \theta \exp \frac{\Delta E}{RT} \tag{4}$$

where t is the reaction time required to accomplish the weight loss at θ when a constant temperature is maintained (for construction of hypothetical isothermal plots of x vs. t) [22]:

$$k = A \exp \frac{\Delta E}{RT}, \tag{5}$$

for determination of k by substitution for T at given A and ΔE values.

In view of the rather high heating rates (ϕ=10–50°C) applied, credibility of the kinetic analysis data thus obtained was checked on by the linearity of automatically monitored ($\Delta T/\Delta t$) vs. T plots. This excludes the possibility of having the linear heating programme distorted by the fast heating, a result that could well be expected on the basis of the minute amount of soot (2±1 mg) and the inclusion of SiC.

3. Results and discussion

3.1. XRD and IR examination of the test catalysts

Table 1 summarizes XRD results, and indicates, accordingly, that the crystalline bulk structure of molybdena is solely composed of MoO_3 crystallites. It also indicates that $BiMoO_x$ and $CrMoO_x$ assume crystalline bulk structures of the corresponding

Table 1
Observed and reference XRD results of molybdena and molybdates

Test material	Observed		Reference			Remarks
	d (nm)	*I*/*I*°	*d* (nm)	*I*/*I*°	Material	
MoO_3	0.3262	100	0.3259	100	MoO_3	Strongly crystallized
	0.3813	76	0.3807	77	Molybdite	
	0.3469	38	0.3462	38	Orthorhombic	
					JCPDS: 35-0609	
$BiMoO_x$	0.3188	100	0.3190	100	$Bi_2Mo_3O_{12}$	Strongly crystallized
	0.3059	91	0.3059	90	Monoclinic	
	0.2881	87	0.2878	85	JCPDS: 21-0103	
$CrMoO_x$	0.3846	100	0.3839	100	$Cr_2Mo_3O_{12}$	Moderately crystallized
	0.3434	77	0.3439	80	Orthorhombic	
	0.3227	59	0.3230	60	JCPDS: 20-0310	
$BaMoO_x$	0.3356	100	0.3357	100	$BaMoO_4$	Strongly crystallized, and contains a minor proportion of poorly crystallized $BaO_2{\cdot}8H_2O$ (JCPDS: 3-0306)
	0.3209	23	0.2788	25	Tetragonal	
	0.2103	30	0.2104	30	JCPDS: 29-0193	
$MnMoO_x$	0.3452	100	0.3451	100	$MnMoO_4$	Poorly crystallized
	0.3890	45	0.3889	40	Monoclinic	
	0.3335	18	0.3330	16	JCPDS: 27-1280	
$CuMoO_x$	0.3442	100	0.3439	100	$Cu_3Mo_2O_9$	Moderately crystallized, and may contain molybdate monomers
	0.3322	88	0.3298	87	Orthorhombic	
	0.3519	78	0.3528	76	JCPDS: 24-0055	

molybdates, i.e. $Bi_2Mo_3O_{12}$ and $Cr_2Mo_3O_{12}$, respectively, with the former being more crystalline than the latter. As for the $BaMoO_x$, $MnMoO_x$ and $CuMoO_x$, the table shows the former to have a well crystalline bulk structure constituting dominantly $BaMoO_4$ and a minor proportion of a separate $BaO_2{\cdot}8H_2O$ phase, the latter to contain moderately crystalline $Cu_3Mo_2O_9$ and likely monomolybdates ($CuMoO_4$), and the $MnMoO_x$ to exhibit a weak XRD pattern due to $MnMoO_4$.

Table 2 demonstrates frequencies and assignments of IR absorptions displayed in the spectra taken from the test materials over the Mo–O vibration frequency region ($\leq 1000\ cm^{-1}$). The results indicate that (i) MoO_3 only constitutes molybdate tetrahedra, (ii) $Bi_2Mo_3O_{12}$ assumes the α-form and may contain molybdate tetrahedra and octahedra, (ii) $Cr_2Mo_3O_{12}$ assumes the ß-form, which may account for the presence of some $Cr_2Mo_2O_9$, (iii) $BaMoO_4$ exists in the τ-form and contains minority of barium carbonate, (iv) $MnMoO_4$ exists largely in a polymeric form and may include non-crystalline MnO_x species, and (v) $Cu_3Mo_2O_9$ may exist in a multi-phasic composition containing the α-, ß- and τ-forms.

3.2. Soot oxidation on molybdena vs. chromia and tungsta

TG curve (c, Fig. 1) obtained for a mixture of (2.7 mg soot+57.3 mg SiC) displays a single weight

Table 2
Observed frequencies (cm^{-1}) and assignments (based on [23], and references therein) of IR absorptions monitored for molybdena and molybdates

Test material	νMo=O	ν_{as}Mo–O–Mo	ν_{S}Mo–O–Mo	δMo=O	Remarks
MoO_3	992 (s)	877 (s,b)	612 (s,vb)	485 (m,sh)	Corner sharing $(MoO_4)^{2-}$ tetrahedra in layer-structured MoO_3
		820 (sp,sh)	512 (m,sh)		
$BiMoO_x$	985 (vw)	852 (vs,b)	676 (s)	467 (m)	Diagnostic to α-form of $Bi_2Mo_3O_{12}$, and may account for presence of $(MoO_4)^{2-}$ and $(MoO_6)^{-}$
	934 (s)	833 (s,sh)	579 (s)	438 (m)	
	903 (s)	717 (s)	550 (s,sh)		
$CrMoO_x$	993 (vw)	869 (s,b)	603 (w,b)	429 (w)	Diagnostic to ß-form of $Cr_2Mo_3O_{12}$, which may account for presence of some $Cr_2Mo_2O_9$
	971 (w)	820 (s,sh)		405 (w)	
	930 (m)				
$BaMoO_x$	927 (s)	855 (s)	681 (s,b)	472 (w)	Consistent with $BaMoO_4$ in τ-form, i.e. Ba_3MoO_6 like. Two bands at 1417 and 1361 cm^{-1} may be associated with the XRD detected BaO_2 species, which is accordingly rather carbonate than oxide
	905 (s)	825 (vs,b)	585 (m)	447 (w)	
		774 (w)	558 (m,sh)		
		755 (w)	520 (w,sh)		
$MnMoO_4$	943 (s)	868 (m)	653 (s,b)	401 (s,b)	Account for the XRD-detected $MnMoO_4$, however, in a polymeric form. Strong absorptions at 750–400 cm^{-1} may conceal bands due to separate MnO_x species
	929 (s,sh)	799 (m)	618 (vs)		
		710 (s,b)	533 (m,sh)		
$CuMoO_x$	963 (s)	875 (s,b)	530 (w,sh)	460 (w,sh)	Account not only for the XRD detected $Cu_3Mo_2O_9$ (ß-form), but also for a multiphasic composition that might accomodate both α- and γ-type of species
	940 (s,sh)	845 (s,sh)	496 (s)	428 (vw)	
	904 (m)	826 (m,sh)			
		802 (m,sh)			
		722 (s,b)			

Line shapes; vs: very strong, s: strong, sp: sharp, b: broad, m: medium, sh: shoulder, w: weak, and vw: very weak.

loss (WL) step maximized at T_{max}=571°C. The WL determined (~4.5%) amounts to the complete oxidation (combustion) of the amount of soot contained into CO_2(g), since SiC has been found weight-invariant over the temperature range scanned (up to 700°C). Therefore, the temperature at which the rate of the oxidation process is maximized, i.e. T_{max}, will be called now onwards 'soot ignition temperature'.

The TG curves (d and e) given in Fig. 1 reveal that the presence of Cr_2O_3 in the 'SiC+soot' mixture decreases slightly the ignition temperature to 523°C, and that of MoO_3 does likewise but consider-

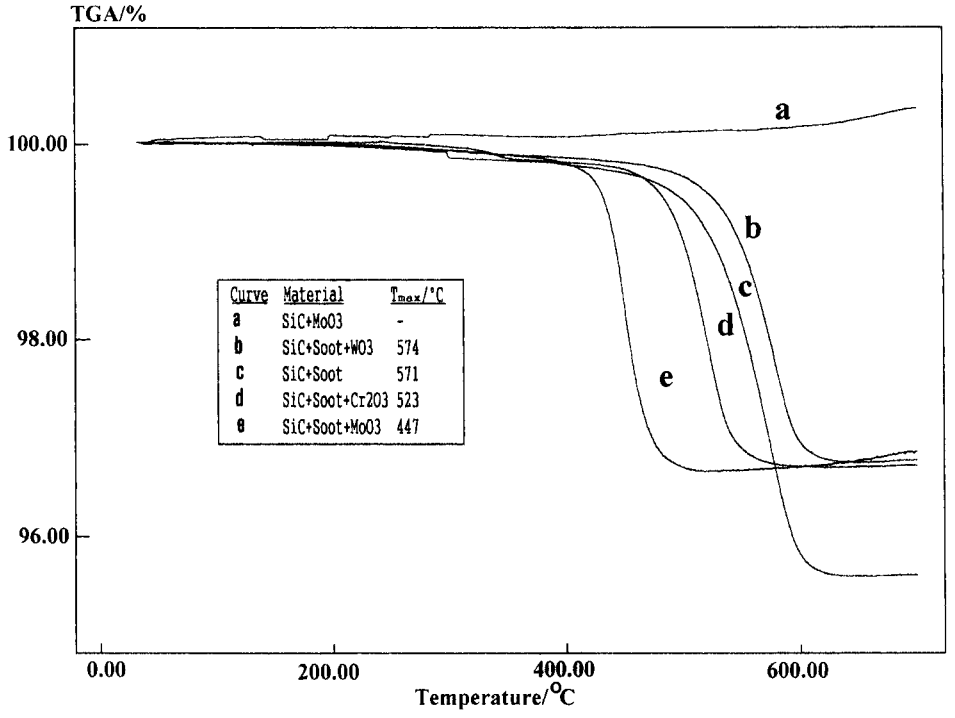

Fig. 1. TG curves obtained on heating (at 10°C/min) of the materials indicated in 50 cm^3 air/min.

ably to 447°C. In contrast, the TG curve (b, Fig. 1) obtained for the mixture of 'SiC+soot+WO_3' indicates that the addition of WO_3 does not decrease the soot ignition temperature. The WL determined (~3.3%) in the three curves (b, d and e) is due only to the combustion of soot (~2 mg), since the three oxides were found to be weight-invariant in the temperature range examined. As for example, the TG curve obtained for 'SiC+MoO_3' is also given in Fig. 1 (curve a).

The above results clearly show that molybdena is a much better catalyst of soot combustion than chromia, whereas tungsta does not show a detectable activity in the reaction. If the active catalytic behaviour of molybdena vs. chromia may be attributed to the much higher volatility (mobility) of MoO_3 ($\Delta G_f^0 = -668$ kJ/mol) than Cr_2O_3 ($\Delta G_f^0 = -1058$ kJ/mol), the slightly lower volatility of WO_3 ($\Delta G_f^0 = -764$ kJ/mol) [24] than MoO_3 cannot be allocated fully the responsibility of the inactive catalytic behaviour of tungsta as compared to both molybdena and chromia (Fig. 1). There must have been other important reasons, which might include unfavourable characteristics of redox conduct of W(VI)–O species.

3.3. Soot oxidation on molybdates

Fig. 2 compares TG curves obtained for the SiC + soot mixtures containing the molybdates and MoO_3 with that containing neither of these materials. All of these curves show a single WL-step occurring at <600°C, except for that of the $BaMoO_x$-containing mixture which monitors an additional, slight WL-step maximized at 586°C. The slight WL effected (0.3%) via this additional step is most likely associated with the decomposition of the minority, separate barium compound (whether $BaO_2 \cdot 8H_2O$, or $BaCO_3$) contained in the catalyst material.

It is obvious from Fig. 2 that all of the molybdates tested could catalyze the combustion of soot, except for $MnMoO_x$ which shows an insignificant effect. However, the sole molybdate which could surpass the catalytic conduct of MoO_3 is $CuMoO_x$. This is

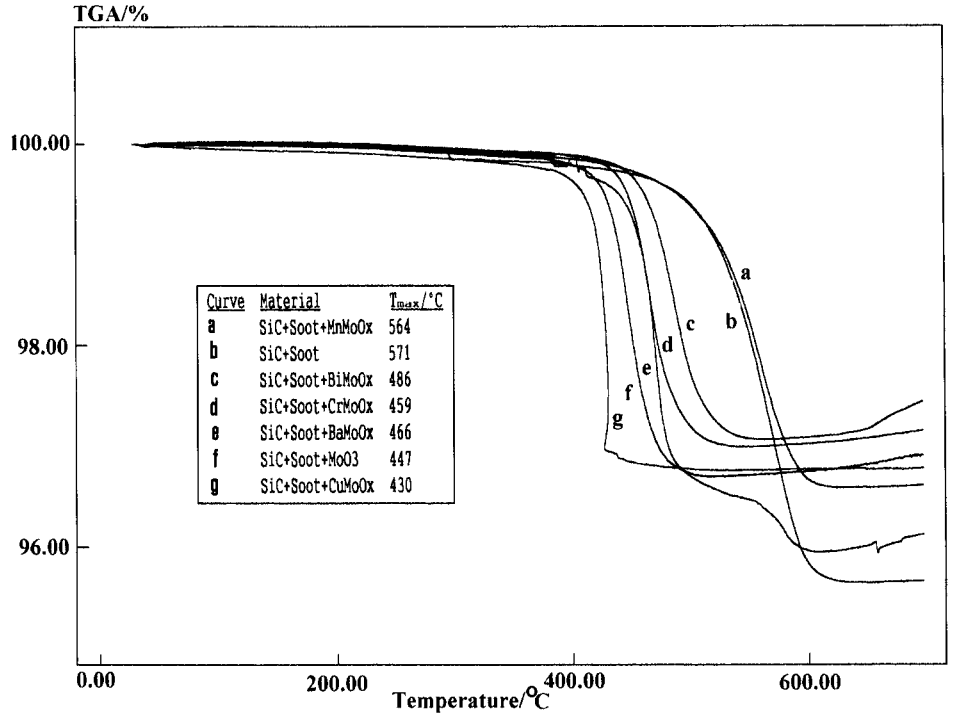

Fig. 2. TG curves obtained on heating (at 10°C/min) of the materials indicated in 50 cm^3 air/min.

shown by the lower soot ignition temperature effected by $CuMoO_x$ (=430°C) than that effected by MoO_3 (=447°C). Thus, in the presence of $CuMoO_x$ the ignition temperature of soot is brought into the exhaust temperature range (200–450°C) of diesel-run engines [7]. $CuMoO_x$ is, accordingly, as reactive as unsupported (T_{max}=350–420°C) and ZrO_2-supported (T_{max}=400°C), KCl-promoted $CuMoO_4$ [7] which are 'tight contact' soot oxidation catalysts. Though the volatility (mobility) of $CuMoO_x$ (ΔG_f^0=−810 kJ/mol) is markedly higher than that of the other test molybdates (ΔG_f^0=−1091 to −1439 kJ/mol) [24], it is relatively lower than that of MoO_3 (ΔG_f^0=−668 kJ/mol) [24]. Thus, it is probably the multi-phasic nature of $CuMoO_x$ (Table 2) and copper-promoted favourable electronic environment that sustain the high catalytic activity shown by the material.

It is worth reporting, at this stage, that neither of the thermal behaviours observed for the test reaction mixtures, whether catalyzed or uncatalyzed, has been influenced by changing the heating atmosphere form dry to wet air. Hence, the presence of water molecules in the reaction atmosphere, which is known to promote the volatility of molybdena species ($MoO_3(s)+H_2O(g)\rightarrow MoO_2(OH)_2(g)$, [14]), seems not to be of importance to the catalytic conduct of the test materials in soot oxidation.

3.4. Kinetics of uncatalyzed vs. catalyzed soot oxidation

Fig. 3 displays non-isothermal (Fig. 3(A) and (B)) and hypothetically isothermal (Fig. 3(C) and (D)) kinetic analysis results of the uncatalyzed combustion of soot. The kinetic parameters therefrom derived are compared to those derived for the catalyzed combustion by MoO_3 and $CuMoO_x$ in Table 3. It is obvious from the table that the oxidation of soot, whether catalyzed or uncatalyzed, is nearly a first order process. MoO_3 decreases the activation energy of the process from 247 to 209 kJ/mol, and $CuMoO_x$ further decreases to 163 kJ/mol, thus confirming the catalytic effects of these materials.

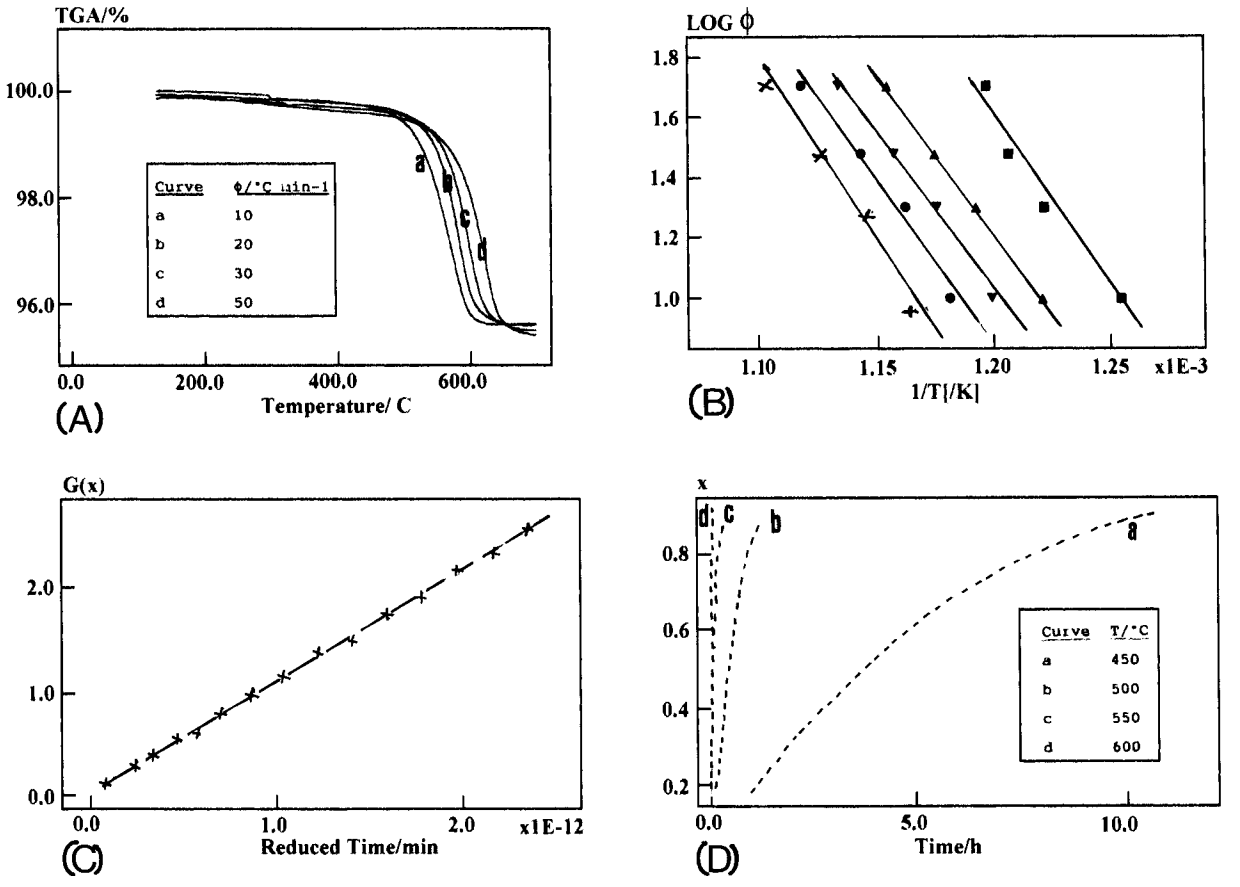

Fig. 3. Non-isothermal (A and B) and hypothetically isothermal (C and D) kinetic analysis of uncatalyzed oxidation (combustion) of soot in a dynamic atmosphere of air (curves in C and D are reconstructed with the help of Eqs. (2)–(4)).

The catalytic oxidation of soot by metal oxides is often thought to proceed through a redox mechanism [7]:

$2MO_n + C \rightarrow CO_2 + 2MO_{n-1}$, ... metal oxide reduction (1)

$2MO_{n-1} + O_2 \rightarrow 2MO_n$, ... metal oxide oxidation (2)

In this mechanism, the tightness of contact between soot and the metal oxide and the strength of the metal–oxygen bond are important parameters. With respect to the present catalysts, a tight contact with soot particulates may be realized by solid/solid wetting [25] at MoO_x/C interfaces and/or gas phase transport of $MoO_2(OH)_2$ species [26]. On basis of the present results, water molecules in the surrounding atmosphere play no role in the thermal behaviour of the catalytic materials. This supports the views of Margraf et al. [27] who reported that the solid/solid wetting mechanism is much more likely than the gas phase transport mechanism. The solid/solid wetting at MoO_x/C interfaces is sustained by the high mobility of the molybdate species. Thus, the relatively higher mobility of MoO_3 and $CuMoO_x$ can warrant tighter contacts between the catalytic species and soot particulates, than the other test catalysts (Table 1). The importance of tight contacts is also true comparing the catalytic conducts of $BaMoO_x$, $BiMoO_x$, $MnMoO_x$ and $CrMoO_x$ with MoO_3, since the redox kinetics of the five materials is similarly determined by the more difficult reduction step of Mo(VI) than the oxidation step of lower valent Mo ions [28]. The counter cations of the indicated molybdates cannot

Table 3
Kinetic parameters for uncatalyzed and catalyzed combustion of soot in a dynamic atmosphere of air, as derived using the mathematical apparatus of Ozawa's method [20–22]

Reaction mixture	Activation[a] energy (ΔE kJ mol^{-1})	Reaction order (n)	Frequency factor (A min^{-1})	Rate constant	
				Temperature (°C)	k (min^{-1})
SiC+Soot	245	~1.0	1.9×10^{18}	450	4.6×10^{13}
				500	9.5×10^{13}
				550	1.8×10^{14}
				600	5.2×10^{14}
SiC+Soot+MoO_3	209	0.9	4.4×10^{15}	400	1.6×10^{11}
				450	3.0×10^{11}
				500	5.2×10^{11}
				550	1.9×10^{12}
SiC+Soot+$CuMoO_x$	163	0.8	2.8×10^{9}	400	7.0×10^{6}
				450	1.0×10^{7}
				500	1.4×10^{7}
				550	1.9×10^{7}

[a] It is the average value of the activation energy values determined at different reaction conversions, according to Ozawa's method [20–22].

promote the difficult reduction of Mo(VI), because all of them, (Ba(II), Mn(II), Bi(III) and Cr(III)) are also difficult to reduce. In contrast is the case, when the catalytic conduct of $CuMoO_x$ is compared with that of MoO_3. $CuMoO_x$ is less volatile than MoO_3 [24], yet it is more active in soot oxidation (Fig. 2 and Table 3). Hence, the decisive role will be that of the redox behaviour: (i) reduction of Cu(II)–O species by soot (carbon), (ii) formation of CO_2(g), (iii) electron transfer from the resulting Cu(I) to Mo(VI)–O with consequent oxygen spill-over to copper (i.e., restoration of Cu(II)–O species, and (iv) oxidation of Mo(V)–O thus generated by the surrounding O_2 (g). Thus, the difficult reduction of Mo(VI) species in $CuMoO_x$ is promoted by the facile reduction of Cu(II) [29], and the difficult oxidation of Cu(I) will be promoted by the facile oxidation of Mo(V) and, consequently, the overall kinetics of the reaction. This may provide a plausible explanation for the highest soot oxidation activity exhibited by $CuMoO_x$ (Fig. 2 and Table 3) as compared to the other test catalysts.

4. Conclusions

Molybdena (MoO_3) and copper molybdate ($Cu_3Mo_2O_9$) are competent soot oxidation catalysts in air. They are capable of lowering the ignition temperature of soot (571°C) to 447°C (MoO_3) and further to 430°C ($Cu_3Mo_2O_9$), i.e. to occur eventually in the temperature range of the exhaust of diesel-powered combustion engines (200–450°C). The accomplishment of such high oxidation activity without promotion with chloride additives [7,12,13] promises more durable catalysts than the promoted ones [7] and eliminates the environmental risk associated with formation of copper(oxy)chlorides [7].

Acknowledgements

The financial support of Kuwait University via research projects No. SC076, SLC063, and the excellent technical assistance at Analab/SAF of the Chemistry Department, are highly appreciated.

References

[1] K. Taylor, in: J.R. Anderson, M. Boudart (Eds.), Catalysis Science and Technology, Springer, Berlin, vol. 5, 1984, pp. 119–170.
[2] R. Prasad, L.A. Kennedy, E. Ruckenstein, Catal. Rev. -Sci. Eng. 26 (1984) 1.

[3] F. Nakajima, Catal. Today 10 (1991) 1.
[4] J.P.A. Neeft, M. Makkee, J.A. Moulijn, Appl. Catal. B 8 (1996) 57.
[5] W.F. Shangguan, Y. Teraoka, S. Kagawa, Appl. Catal. B 8 (1996) 217.
[6] W.F. Shangguan, Y. Teraoka, S. Kagawa, Appl. Catal. B 12 (1997) 237.
[7] G. Mul, J.P.A. Neeft, F. Kapteijn, M. Makkee, J.A. Moulijn, Appl. Catal. B 6 (1995) 339.
[8] M.I. Zaki, G. Kunzmann, B.C. Gates, H. Knözinger, J. Phys. Chem. 91 (1987) 1486.
[9] M.I. Zaki, T.H. Ballinger, J.T. Yates Jr., , J. Phys. Chem. 95 (1991) 4028.
[10] E.S. Lox, B.H. Engler, E. Koberstein, Studies Surf. Sci. Catal. 71 (1991) 291.
[11] A.F. Ablström, C.U.I. Odenbrand, Appl. Catal. 60 (1990) 157.
[12] P. Ciambelli, M. D'Amore, V. Palma, S. Vaccaro, Combustion Flame 99 (1994) 413.
[13] Y. Watabe, C. Yamada, K. Irako, Y. Murakami, Catalyst for Use in Cleaning Exhaust Gas Particulates, Eur. Pat. Appl., 0092023, 1983.
[14] O. Glemser, R. von Hässeler, Z. Anorg. Allg. Chem. 316 (1962) 168.
[15] G. Mestl, B. Herzog, R. Schlögl, H. Knözinger, Langmuir 11 (1995) 3027.
[16] G. Mestl, N.F.D. Verbruggen, E. Bosch, H. Knözinger, Langmuir 12 (1996) 2961.
[17] P.J. Gellings, H.J.M. Bouwmeester, Catal. Today 12 (1992) 1.
[18] A. Bielanski, J. Haber, Oxygen in Catalysis, Marcel Dekker, New York, 1991.
[19] M.I. Zaki, H.M. Ismail, R.B. Fahim, Surface Interface Anal. 8 (1986) 185.
[20] T. Ozawa, Bull. Chem. Soc. Japan 38 (1965) 1881.
[21] T. Ozawa, J. Thermal Anal. 2 (1970) 301.
[22] T. Ozawa, Thermochim. Acta 203 (1992) 159.
[23] G. Mestl, H. Knözinger, in: G. Ertl, H. Knözinger, J. Weitkamp (Eds.), Handbook of Heterogenous Catalysis, vol. 2, Wiley-VCH, Weinheim, Germany, 1997, pp. 539–574.
[24] I. Barin, Thermochemical Data of Pure Substances, Part I and II, VCH, Weinheim, 1993.
[25] J. Haber, T. Machej, T. Czeppe, Surf. Sci. 151 (1985) 301.
[26] J. Leyrer, M.I. Zaki, H. Knözinger, J. Phys. Chem. 90 (1986) 4775.
[27] R. Margaraf, J. Leyrer, E. Taglauer, H. Knözinger, React. Kinet. Catal. Lett. 35 (1987) 261.
[28] M.I. Zaki, B. Vielhaber, H. Knözinger, J. Phys. Chem. 9 (1986) 3176.
[29] F. Severino, J. Brito, O. Carios, J. Laine, J. Catal. 102 (1986) 172.